

Fermi surface change across a deconfined quantum critical point

Ribhu K. Kaul,¹ Alexei Kolezhuk,^{1,2} Michael Levin,¹ Subir Sachdev,¹ and T. Senthil^{3,4}

¹*Department of Physics, Harvard University, Cambridge MA 02138*

²*Institut für Theoretische Physik, Universität Hannover, 30167 Hannover, Germany*

³*Center for Condensed Matter Theory, Department of Physics,
Indian Institute of Science, Bangalore 560 012, India*

⁴*Department of Physics, Massachusetts Institute of Technology, Cambridge MA 02139*

(Dated: May 25, 2019)

Abstract

The quantum phase transitions of metals have been extensively studied in the rare-earth “heavy electron” materials, the cuprates, and related compounds¹. The Fermi surface of the metal often has different shapes in the states well away from the critical point. It has been proposed^{1,2,3} that these differences can persist up to the critical point, setting up a discontinuous Fermi surface change across a continuous quantum transition. We study square lattice antiferromagnets undergoing a continuous transition from a Néel state to a valence bond solid, and examine the fate of a small density of holes in the two phases. Fermi surfaces of charge e , spin 1/2 quasiparticles appear in both phases, enclosing the usual Luttinger area. However, additional quantum numbers cause the area enclosed by each Fermi surface pocket to jump by a factor of 2 across the transition in the limit of small density. We demonstrate that the electronic spectrum across this transition is described by a critical theory of a localized impurity coupled to a 2+1 dimensional conformal field theory. This critical theory also controls the more complex Fermi surface crossover at fixed density, which likely involves intermediate phases with exotic fractionalized excitations. We suggest that such theories control the electronic spectrum in the pseudogap phase of the cuprates⁴.

I. INTRODUCTION

Many strong correlation problems of current interest relate to the physics of doped Mott insulators. Most observed metallic states can be understood in conventional terms: ordering associated with broken spin or lattice symmetries, along with Fermi surfaces of charge e , spin 1/2 quasiparticles. Nevertheless, the details of the state differ depending upon the importance we attach to strong correlation physics *e.g.* different Fermi surface topologies and magnetic moment configurations are obtained from the weak and strong interaction limits, namely (*i*) a spin density wave instability of the free electron band structure, or (*ii*) a spin-wave theory of a lightly doped magnetically ordered Mott insulator. It is clear that rich physics lies in understanding the interpolation between such limiting regimes, and that there are a number of important applications *e.g.* to the widely discussed differences between the underdoped and overdoped cuprates.

A central question is whether there could be a single continuous quantum phase transition between such states with distinct types of order or Fermi surface topologies (recent experiments⁵ on CeRhIn₅ are compatible with an abrupt or very rapid change in Fermi surface topology). Such critical points could be the key to understanding the many observed ‘non-Fermi liquid’ properties. However, a complete critical field theory of a continuous transition between such states has so far been presented only in insulators⁶, where the two states have broken symmetries which cannot be connected by a continuous transition in Landau theory; instead a ‘deconfined’ theory focussing not on order parameters but on fractionalized excitations and emergent gauge forces shows that such transitions are indeed possible. An extension of these ideas to metallic systems has been discussed^{3,7}, including a scenario which would allow for a discontinuous change in a Fermi surface. Others⁸ have proposed a ‘local quantum critical’ scenario for transitions between states with different Fermi surface topologies, based upon numerical studies in extensions to dynamic mean field theory. However, the analytic structure of this mean field transition remains unclear, and it is not clear how, even in principle, this ‘local critical’ structure can be extended beyond mean field theory.

In this paper, we will build on the theory of the deconfined quantum critical point proposed in Ref. 6 for insulating spin $S = 1/2$ antiferromagnets on the square lattice^{10,11,12,13}, the transition is between (see Fig. 1) a state with magnetic Néel order (with spin polarized in the staggered configuration) to a spin-gap state with valence bond solid (VBS) order (which

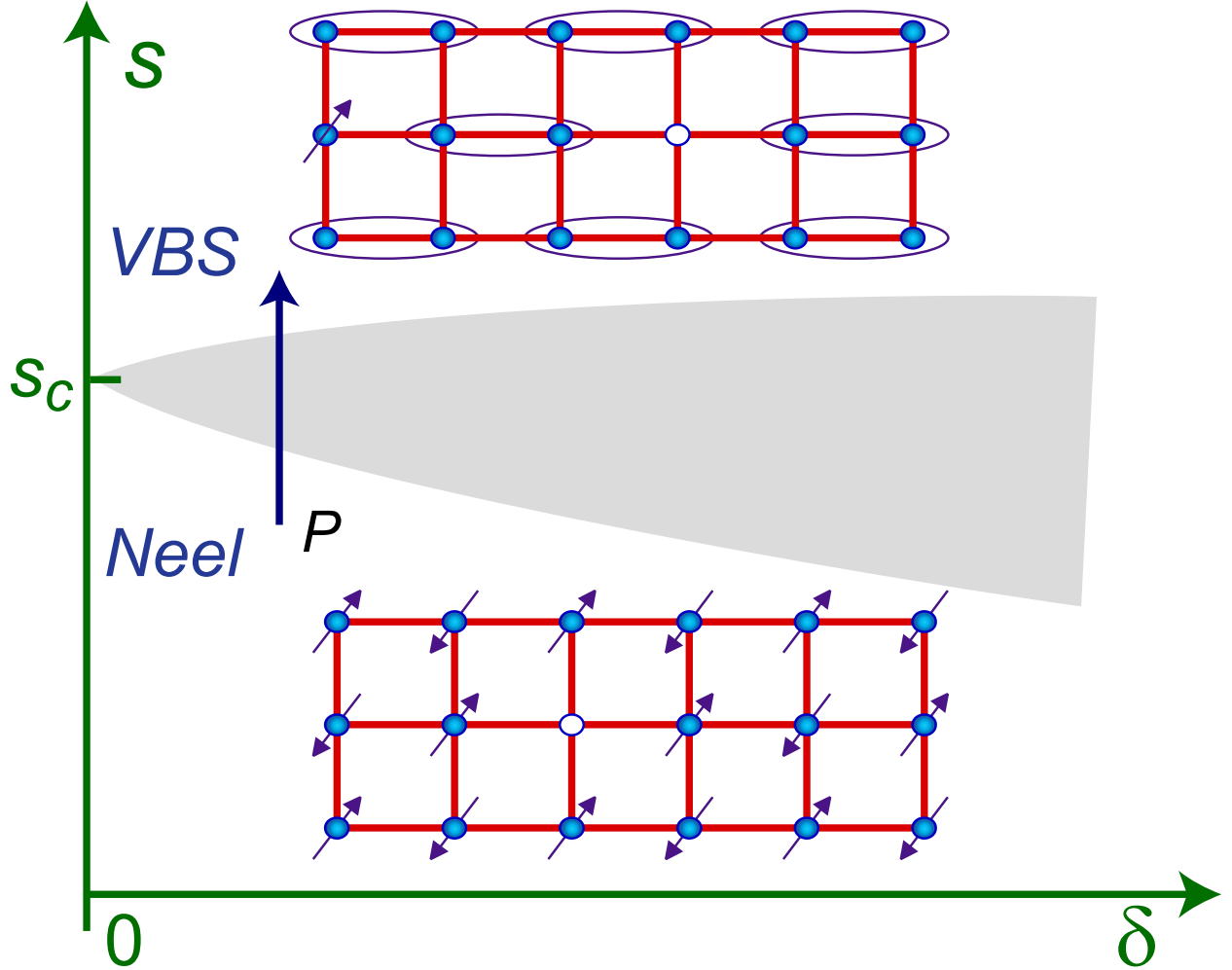


FIG. 1: Schematic phase diagram. The ellipses represent spin singlet valence bonds. The coupling s tunes the insulator across the Néel-VBS transition, and δ is the mobile hole density. The deconfined quantum critical point is at $s = s_c$ in the insulator with $\delta = 0$. The vacancies ('holons') carry a gauge charge $q = \pm 1$ under an emergent $U(1)$ gauge force. In the cartoons above, the reader can interpret q as a sublattice label. In the $s < s_c$, Néel phase, q determines the spin: a vacancy on an up (down) spin site carries net spin down (up) and so is equivalent to a charge e spin-1/2 hole. For $s > s_c$, the hole is a composite of a vacancy and a nearby unpaired spin with opposite q , moving by rearranging nearest-neighbor valence bonds; note that this motion preserves spin and sublattice quantum numbers *separately* (see also Ref. 9). So there are twice as many states per momentum for a charge e spin 1/2 hole in the VBS state than there are in the Néel state.

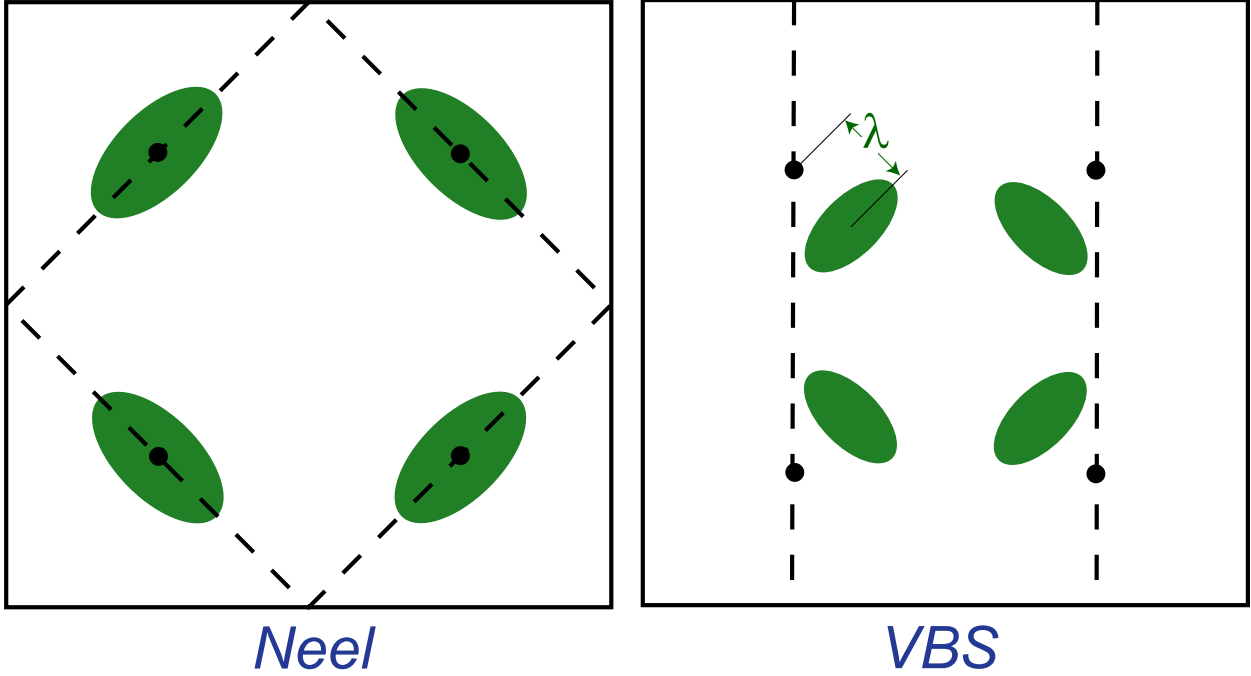


FIG. 2: Momentum space Fermi surfaces in the Néel and VBS regions of Fig 1. The filled circles are the 4 \vec{K}_p wavevectors, with $\vec{K}_1 = (\pi/2a)(1, 1)$, $\vec{K}_2 = (\pi/2a)(1, -1)$, $\vec{K}_3 = -\vec{K}_1$, $\vec{K}_4 = -\vec{K}_2$, with a the lattice spacing. The dashed line in the Néel phase indicates the boundary of the magnetic Brillouin zone. Only the Fermi surfaces within this zone contribute to the Luttinger counting, and so the area of each ellipse is $\mathcal{A}_F = (2\pi)^2\delta/4$. In the VBS phase, all 4 pockets are inequivalent, and so the area of each ellipse is $\mathcal{A}_F = (2\pi)^2\delta/8$. The dashed lines now show the reduction of the Brillouin zone due to the VBS order which appears at sufficiently low temperatures; “shadow” Fermi surfaces, with weak photoemission intensity (estimated in the text), will appear as reflections across these lines, and these Fermi surfaces are not shown.

is spin rotation invariant, but breaks lattice symmetries by ordering of valence bonds). We will describe the metallic states obtained by doping this system with a small density (δ) of holes. Figs. 1 and 2 summarize our key results, and the captions support them with simple physical arguments. The decoupling of the spin and U(1) gauge charge in the VBS phase described in Fig. 1, and the consequent doubling of the hole flavors in Fig. 2, leads to our precise result: the discontinuity in $\lim_{\delta \rightarrow 0} \mathcal{A}_F / \delta$ on the two sides of the Néel-VBS quantum critical point, as shown in Fig. 2.

On the other hand, the evolution of the Fermi surface along the fixed δ line P in Fig 1 involves separate questions associated with the interplay between the mobile holes and the $s = s_c$ deconfined critical point. If the $\delta = 0$ monopole-induced confinement physics⁶ survives for $\delta > 0$, then there will be a single critical line which is crossed by P at which the Fermi surface changes discontinuously. However, this appears unlikely because the monopoles can be screened by the charge carriers¹⁴, leading to a narrow intermediate fractionalized ‘holon metal’ phase with no conventional Fermi surface within the shaded region. In either case, there is a wide momentum, frequency, and temperature regime over which the hole spectral function is incoherent. We will show here that this is described by a universal theory of a single localized vacancy¹⁵ coupled to the 2+1 dimensional conformal field theory of the $\delta = 0$, $s = s_c$ critical point. The incoherent, critical hole spectral function is momentum-independent, and so while this view of the transition has a ‘local’ character⁸, the degrees of freedom include a non-trivial, bulk quantum field theory. Further, we believe that the evolution of the fermionic excitations across the shaded region of Fig 1 cannot be captured by dynamic mean field theory methods or self-consistent impurity models.

II. FIELD THEORY

The motion of charge carriers doped into an insulating square-lattice quantum antiferromagnet is conventionally described by the “ t - J ” model,

$$H_{t-J} = - \sum_{i,j,\sigma} t_{ij} (c_{i\sigma}^\dagger c_{j\sigma} + \text{h.c.}) + \sum_{i,j} J_{ij} \vec{S}_i \cdot \vec{S}_j, \quad (1)$$

where $c_{i\sigma}^\dagger$ creates an electron with spin σ on the sites i of a square lattice and $\vec{S}_i = \frac{1}{2} \sum_{\sigma\sigma'} c_{i\sigma}^\dagger \vec{\sigma}_{\sigma\sigma'} c_{i\sigma'}$. In addition, the constraint $\sum_\sigma c_{i\sigma}^\dagger c_{i\sigma} \leq 1$ is enforced on each site, modelling the large local repulsion between the electrons. It is important to note that our results

are more general than a particular t - J model, and follow almost completely from symmetry considerations.

We begin our analysis by recalling the physics in the absence of doped holes; we then only need to consider the second term in Eq. (1) *i.e.* the ‘Heisenberg model’. With weakly frustrated J_{ij} the ground state is the Néel state. With stronger frustration (or additional ring exchanges), there can be a quantum transition to a VBS phase¹⁷. The field theory for the Néel-VBS transition in the insulator⁶ is expressed in terms of a complex ‘relativistic’ field z_α , where $\alpha = \uparrow, \downarrow$, which is the field operator for a charge neutral, spin $S = 1/2$ spinon excitation. Low lying singlet excitations are represented by an emergent U(1) gauge field A_μ , where $\mu = \tau, x, y$ is a spacetime index. The field theory has the action $\int d^2r d\tau \mathcal{L}_z$ with

$$\mathcal{L}_z = |(\partial_\mu - iA_\mu)z_\alpha|^2 + s|z_\alpha|^2 + \frac{u}{2}(|z_\alpha|^2)^2 + \dots \quad (2)$$

Here s is the tuning parameter in Fig. 1, we have set a spinon velocity to unity, and u is a spinon self-interaction. For $s > s_c$, this field theory is in a spin SU(2)-invariant U(1) spin liquid phase, with gapped spinon excitations, and provides a continuum description of the Schwinger boson mean field theory of the square lattice antiferromagnet¹⁶. The inclusion of monopole tunneling events shows that this spin liquid is ultimately unstable to confinement and the development of VBS order¹⁷. This monopole physics is peripheral to our main results, and so we defer its discussion until later.

Now we need to add charge carriers to this antiferromagnet. We have represented the spin excitations of the antiferromagnet by Schwinger bosons above, and so the charge carriers require a spinless fermion f , the ‘holon’ (see Appendix A for more details). Such a mean-field lattice study has been carried out some time ago in Refs. 18,19. We can take the low energy limit of their results, and so obtain the field theory needed for our analysis. However, we can also proceed on symmetry grounds, when our main ingredients are the transformation properties of the various fields under square lattice symmetry operations. Because the elementary quanta also carry U(1) gauge charges, it is not required that the fields be invariant under such operations, only their gauge-invariant combinations. This larger space of transformations was dubbed the projective symmetry group (PSG) by Wen²⁰, and we list the PSG of the z_α in Table I. This f holon also carries the gauge charge of the U(1) gauge field A_μ in Eq. (2). Indeed, because the spinon field flips charges under a sublattice interchange in Table I, we see that holons on the two sublattices have charges $q = \pm 1$. This q

	T_x	$R_{\pi/2}^{\text{dual}}$	I_x^{dual}	\mathcal{T}
z_α	$\varepsilon_{\alpha\beta} z^{\beta*}$	$\varepsilon_{\alpha\beta} z^{\beta*}$	$\varepsilon_{\alpha\beta} z^{\beta*}$	$\varepsilon_{\alpha\beta} z^\beta$
f_{+1}	if_{-1}	if_{-2}	if_{-2}	f_{+1}
f_{-1}	$-if_{+1}$	if_{+2}	if_{+2}	$-f_{-1}$
f_{+2}	if_{-2}	if_{-1}	if_{-1}	f_{+2}
f_{-2}	$-if_{+2}$	$-if_{+1}$	if_{+1}	$-f_{-2}$
Φ_{VBS}	$-\Phi_{\text{VBS}}^*$	$i\Phi_{\text{VBS}}^*$	Φ_{VBS}	Φ_{VBS}

TABLE I: PSG transformations of the fields under square lattice symmetry operations. T_x : translation by one lattice spacing along the x direction; $R_{\pi/2}^{\text{dual}}$: 90° rotation about a dual lattice site on the plaquette center ($x \rightarrow y, y \rightarrow -x$); I_x^{dual} : reflection about the dual lattice y axis ($x \rightarrow -x, y \rightarrow y$); \mathcal{T} : time-reversal, defined in real time. $\varepsilon_{\alpha\beta}$ is the antisymmetric tensor with $\varepsilon_{\uparrow\downarrow} = 1$ and $\varepsilon_{\alpha\beta} = \varepsilon^{\alpha\beta}$. The local VBS order parameter is defined as $\Phi_{\text{VBS}}(\vec{r}) \equiv (-1)^{\vec{r} \cdot \hat{x}} \langle S_{\vec{r}} \cdot S_{\vec{r} + \hat{x}} \rangle + i(-1)^{\vec{r} \cdot \hat{y}} \langle S_{\vec{r}} \cdot S_{\vec{r} + \hat{y}} \rangle$; where \hat{x}, \hat{y} are the unit lattice vectors.

quantum number will play a central role. However, the holons can also acquire an additional ‘valley’ quantum number if their dispersion minimum is not at the center of the Brillouin zone; we will keep track of this at the cost of some additional bookkeeping. The analysis of the holon Green’s function of the present U(1) spin liquid phase, along the lines of Ref. 19, shows that there are 2 distinct valleys, with labels $v = 1, 2$, and we choose a gauge in which their minima are at wavevectors $\vec{K}_{1,2}$ shown in Fig. 2. Summarizing, we have 4 species of spinless fermions f_{qv} , with U(1) charge $q = \pm 1$, and valleys $v = 1, 2$. All the information we need to construct the effective action and the observable correlations of these fermionic holons is encapsulated in their PSG, which is derived in Appendix A, and is summarized in Table I.

An immediate consequence of the PSG of the z_α and the f_{qv} is that we can write down an expression for the physical charge $-e$, spin-1/2 electron annihilation operator $c_\alpha(\vec{r}) = \sum_{p=1}^4 e^{i\vec{K}_p \cdot \vec{r}} \Psi_{p\alpha}(\vec{r})$ where the \vec{K}_p are defined in Fig. 2 and

$$\begin{aligned} \Psi_{1,3\alpha} &= z_\alpha f_{+1}^\dagger \pm \varepsilon_{\alpha\beta} z^{\beta*} f_{-1}^\dagger \\ \Psi_{2,4\alpha} &= z_\alpha f_{+2}^\dagger \pm \varepsilon_{\alpha\beta} z^{\beta*} f_{-2}^\dagger \end{aligned} \quad (3)$$

These relations will allow us to construct the Fermi surfaces in Fig. 2.

The field theory of the doped antiferromagnet has the Lagrangian is $\mathcal{L} = \mathcal{L}_z + \mathcal{L}_f + \mathcal{L}_c$. The fermionic holon terms are

$$\mathcal{L}_f = \sum_{qv} f_{qv}^\dagger \left(\partial_\tau - iqA_\tau - \mu - \frac{(\partial_{\bar{j}} - iqA_{\bar{j}})^2}{2m_{v\bar{j}}} \right) f_{qv}, \quad (4)$$

where \bar{j} extends over \bar{x}, \bar{y} , $m_{1\bar{x}} = m_{2\bar{y}}$ and $m_{2\bar{x}} = m_{1\bar{y}}$ are the mass of the elliptical hole pockets, μ is the hole chemical potential, and the \bar{x} and \bar{y} directions are rotated by 45° from the principle square axes. The PSG prohibits a linear derivative term in Eq. (4), and so the f_{qv} dispersion is an extremum at zero momentum; this pins the Fermi surfaces to be centered at \vec{K}_p in the Néel phase (Fig. 2), but not, as we will see, in the VBS phase. Finally, we include coupling between the holons and spinons invariant under all PSG operations. There is an unimportant scalar coupling $\sum_{\alpha qv} |z_\alpha|^2 f_{qv}^\dagger f_{qv}$, but the more important term is

$$\mathcal{L}_c = i\tilde{\lambda}\varepsilon^{\alpha\beta} \left\{ f_{+1}^\dagger f_{-1} z_\alpha \partial_{\bar{x}} z_\beta + f_{+2}^\dagger f_{-2} z_\alpha \partial_{\bar{y}} z_\beta \right\} + \text{c.c.}, \quad (5)$$

equivalent to the dipole coupling introduced by Shraiman and Siggia²¹, arising from the hopping of electrons between nearest-neighbor sites. Another symmetry-based derivation of the theory of the doped antiferromagnet was recently given²² for the Néel phase alone. In contrast, our analysis starting from a spin rotation invariant spin liquid can address the quantum critical point, and can also be specialized to the Néel state by spontaneously breaking spin rotation symmetry. We now turn to an analysis of the motion of holes in the field theory $\mathcal{L} = \mathcal{L}_z + \mathcal{L}_f + \mathcal{L}_c$, first in the Néel and VBS phases, and then finally at the deconfined quantum critical point that separates these two phases.

III. DOPING THE NÉEL STATE

First, consider the $s < s_c$ Néel phase of \mathcal{L}_z with $\langle z_\alpha \rangle \neq 0$. By the Higgs mechanism, the condensate of z_α renders the A_μ massive, and so we can safely integrate the A_μ out. A crucial point is that the Higgs mechanism also ties the U(1) gauge charge q of the holons to the spin quantum number S_z along the Néel order (because of the broken symmetry, S_x and S_y are not conserved); more precisely $S_z = q/2$, and so the f_{qv} carry all the quantum numbers of the electron. This is established in Appendix B.

Now we consider the Fermi liquid state obtained with a total density δ of the four fermion species f_{qv} . Each will form a separate Fermi surface containing $\delta/4$ states; their coupling to the spin-wave can be treated perturbatively, and do not modify any of the key Fermi liquid characteristics. From Eq. (3) we deduce that there are 4 hole pockets centered at the \vec{K}_p wavevectors, each enclosing the area $\mathcal{A}_F = (2\pi)^2(\delta/4)$, as shown in Fig. 2. The caption of Fig. 2 shows that the same area is obtained in direct Fermi liquid counting of electrons within the magnetic Brillouin zone.

IV. DOPING THE VBS STATE

Next, we examine doping the $s > s_c$ state. For now, we neglect monopoles, and so the undoped state is a spin rotation invariant $U(1)$ spin liquid with A_μ representing a gapless ‘photon’ excitation; the spinful excitations are gapped, but single $S = 1/2$ spinons do not exist as asymptotic states—the logarithmic ‘electrostatic’ potential mediated by the A_τ binds the spinons in pairs. We can identify 2Δ as the gap towards creating the lowest spinful excitation; this vanishes at the quantum critical point as $\Delta \sim |s - s_c|^\nu$. In a theory with N spinon species ($\alpha = 1 \dots N$ in Eq. (2)), the logarithmic potential will have the form $V(r) = (12\Delta/N) \ln(r\Delta)$ in the large N limit²³. Now add a single holon into this state. The coupling to A_τ causes this hole to have an ‘electrostatic’ self energy which diverges logarithmically with system size¹⁵, and so a spin-singlet single holon state is not stable. Rather, the holon will peel off a single spinon from above spinon gap, and form a $S = 1/2$, charge e bound state¹⁵. This bound state has the same quantum numbers of as an ordinary hole, and is neutral under the A_μ $U(1)$ gauge force. A finite density of such bound states can then form a Fermi surface with charge e $S = 1/2$ quasiparticles. We also have to consider the pairing between holons with opposite $U(1)$ gauge charges, induced by the A_μ gauge force (this attractive force must be balanced against the repulsive Coulomb force associated with the physical electromagnetic charge e of each holon). This is expected to lead to superconductivity at low enough temperatures, but we will not discuss this here; our focus is on the normal state.

The structure of the holon-spinon bound state is described in more detail in Appendix C. As a consequence of the mixing between the different bound states induced by the terms in \mathcal{L}_c , the bound state eigenmodes turn out to be precisely the electron-like momentum

eigenstates in Eq. (3), with a dispersion which has a minimum at $K_{\bar{x}} = \pm\lambda$ where $\lambda \sim \tilde{\lambda}\Delta^2$. This is responsible for the shift in the centers of the elliptical hole pockets shown in Fig. 2.

The usual counting argument now allows us to deduce the area of each hole pocket. There are 4 inequivalent pockets, and a factor of 2 degeneracy for spin; so $\mathcal{A}_F = (2\pi)^2(\delta/8)$. The factor of 2 difference from the result obtained in the Néel phase is one of our key results.

The state we have described so far is actually *not* a conventional Fermi liquid: the area enclosed by its Fermi surface is not the same as that of a non-interacting electron gas at the same filling and with the same size of unit cell. In the non-interacting case one would have a Fermi surface area $(2\pi)^2(1 - \delta)/2$. In our case, where the holes were doped on a background spin liquid state with a gapless photon excitation, we obtain that the electron-like area enclosed by the Fermi surface is $(2\pi)^2(1 - \delta/2)$. This state is a *fractionalized Fermi liquid*⁷, obtained here in a single band model, in contrast to its previous appearance in Kondo lattice models.

The instability of the spin liquid to confinement and VBS order induced by monopoles^{6,17}, and the associated halving of the Brillouin zone will finally transform the state into one obeying the conventional Luttinger theorem, with an electron-like area enclosed by the Fermi surface of $(2\pi)^2(1 - \delta)/2$. The VBS order parameter is a complex field, Φ_{VBS} , which is proportional to the monopole creation operator. Its expectation value vanishes upon approaching the critical point as $\langle\Phi_{\text{VBS}}\rangle \sim \Delta^{\beta_{\text{VBS}}/\nu}$. The exponent β_{VBS}/ν is the scaling dimension of the monopole operator, which is expected to be large^{6,23}. We are interested here in the mixing induced by $\langle\Phi_{\text{VBS}}\rangle$ across the reduced Brillouin zone shown in Fig 2. However, because of the shift in the minimum of the holon-spinon bound state dispersion discussed above, this mixing is negligible as long as $\sqrt{\delta} < \lambda \sim \Delta^2$, and so can always be neglected as $\delta \rightarrow 0$. This establishes the Fermi surface structure claimed in Fig. 2.

At larger δ , the hole pockets will cross the dashed lines in Fig. 2, and Bragg reflections will split the Fermi surfaces. We analyze this magnitude of the mixing matrix element in the Hamiltonian, using the PSG of Φ_{VBS} in Table 1, in Appendix D. We find that it has a value $\sim \Delta\langle\Phi_{\text{VBS}}\rangle \sim \Delta^{1+\beta_{\text{VBS}}/\nu}$. This splitting of the Fermi surface is negligible provided the matrix element is smaller than the hole kinetic energy, or $\delta > \Delta^{1+\beta_{\text{VBS}}/\nu}$. Over such a possible regime of larger δ , the basic pictures of Figs. 1 and 2 continue to hold. The photoemission intensity of the “shadow” Fermi surfaces noted in Fig. 2 is proportional to the square of the matrix element or $\sim \Delta^{2(1+\beta_{\text{VBS}}/\nu)}$

V. QUANTUM CRITICALITY AND CONCLUSIONS

To complete the picture, let us address the physics of the shaded region in Fig. 1. Here we have a theory of a finite density of holons f_{qv} interacting with spinons z_α via a $U(1)$ gauge force A_μ . At sufficiently long scales, the holons will ‘Thomas-Fermi’ screen that longitudinal A_τ force, and so obviate the binding into gauge neutral combination. Consequently the spinons and holons remain as relatively well-defined excitations, and we enter a fractionalized holon metal phase. This screening can be prevented if the spacing between the holons ($\sim 1/\sqrt{\delta}$) is larger than the holon-spin binding length $\sim 1/\Delta$, or $\delta < \Delta^2$; this fixes the boundary of the shaded region in Fig. 1. The shaded region will exclude the unshaded region of the VBS phase where the Fermi surface splitting is negligible (discussed in the previous paragraph) provided $\beta_{\text{VBS}} > \nu$, an inequality that holds at least for large N .

We now describe the criticality of the hole spectrum at $s = s_c$. We assume here an observation scale (frequency (ω) or temperature (T)) large enough, or a δ is small enough, so that the holes can be considered one at a time. A key observation about a single hole is that its quadratic dispersion (*i.e.* the terms proportional to $1/(2m_{v\bar{x},\bar{y}})$ in \mathcal{L}_f) is an irrelevant perturbation on the quantum critical point of \mathcal{L}_z which involves excitations which disperse linearly with momentum. Consequently, the hole may be considered localized, and its physics is closely related to the single impurity in a spin liquid problem analyzed in Ref. 15. Here we are interested in the single hole Green’s function and this requires the overlap between states of the spin liquid with and without the impurity. This can be computed by analyzing the quantum critical theory of \mathcal{L}_z coupled to one holon localized at $r = 0$, represented by the r -independent Grassmannian $f(\tau)$:

$$\mathcal{S}_{qc} = \int d^2r d\tau \mathcal{L}_z + \int d\tau f^\dagger \left(\frac{\partial}{\partial \tau} + \varepsilon_0 - iA_\tau(r = 0, \tau) \right) f.$$

Here ε_0 is an arbitrary energy fixing the bottom of the holon band, and, following earlier arguments¹⁵, the only relevant coupling between the ‘impurity’ holon degree of freedom and the bulk degrees of freedom of \mathcal{L}_z is the gauge coupling associated with A_τ . The spectral function of a physical charge e , $S = 1/2$ hole is given by the two-point correlation of the composite operator $z_\alpha f^\dagger$. If this operator has scaling dimension $\eta_h/2$, then the universal critical hole Green’s function, G_h , is independent of wavevector and obeys the scaling form

$$G_h = T^{-(1-\eta_h)} \Phi(\hbar(\omega - \varepsilon_0)/k_B T) \quad (6)$$

where Φ is a universal scaling function. At $T = 0$, we obtain an incoherent spectrum associated with the power-law singularity $G_h \sim (\omega - \epsilon_0)^{-1+\eta_h}$. We have computed η_h by a standard $1/N$ expansion for G_h under the action \mathcal{S}_{qc} and found

$$\eta_h = 1 - \frac{36}{N\pi^2} + \mathcal{O}\left(\frac{1}{N^2}\right) \quad (7)$$

Another perspective on the exponent η_h is obtained by mapping it to an observable in the lattice non-compact CP^1 (NCCP) model studied by Motrunich and Vishwanath¹³. On a three-dimensional cubic lattice with spacetime points j , the model has the complex spinor fields $z_{j\alpha}$ on each lattice site, and a vector potential $A_{j\mu}$ on each link extending along the μ direction from site j . The hole Green's function at imaginary time M_τ (in units of the lattice spacing) is then given by the two-point correlator of the $z_{j\alpha}$ in the time direction along with an intermediate ‘Wilson line’ operator (representing the contribution of the f fermion) which renders the correlator gauge invariant (see also Ref. 24):

$$G_h(M_\tau) = \left\langle z_j^{\alpha*} \exp\left(i \sum_{n=0}^{M_\tau-1} A_{j+n\hat{\tau},\tau}\right) z_{j+M_\tau\hat{\tau},\alpha} \right\rangle_{\text{NCCP}};$$

this is expected to decay as $e^{-\tilde{\epsilon}_0 M_\tau} / M_\tau^{\eta_h}$ for large M_τ at the quantum critical point. The continuum limit of the above correlator was computed by Kleinert and Schakel²⁵ in the $1/N$ expansion: their result agrees with Eq. (7).

This paper has presented a theory for a strongly interacting quantum critical point in a metal. The strong interactions imply scaling of observables as a function of $\hbar\omega/k_B T$, which is often seen experimentally, but is absent in the weak-coupling theory²⁶. The theory has an interesting evolution in the Fermi surface geometry across the transition, which is reminiscent of that found in the solution of self-consistent impurity models⁸. However, the details are different, and can only be addressed in a quantum field-theoretic framework which we have described. This work therefore also serves to place studies of quantum transitions in the ‘dynamical mean field theory’ approach^{8,27} in the field-theoretic context.

The T dependent broadening in the quantum-critical hole spectrum in Eq. (6) has similarities to recent observations in the underdoped cuprates⁴. The dispersion minimum is shifted away from the \vec{K}_p points in Fig. 2, as is the case experimentally, and in contrast to other theories of the normal state based upon Dirac fermion spinons. This suggests that a theory such as ours, based upon a fractionalized Fermi liquid state⁷, should lead to a useful description of the pseudogap phase.

Acknowledgments

We are grateful to M. Metlitski for valuable discussions. This research was supported by the NSF grants DMR-0537077 (SS and RKK), DMR-0132874 (RKK) and DMR-0541988 (RKK). AK was supported by Grant KO2335/1-1 under the Heisenberg Program of Deutsche Forschungsgemeinschaft, ML by the Harvard Society of Fellows, and TS by a DAE-SRC Outstanding Investigator Award in India.

APPENDIX A: DERIVATION OF THE PSG

We are interested here in the physics of the t - J like models in which the Hilbert space is restricted to 3 possible states on each site of the square lattice: an up/down spin electron, and a vacancy. The state with two electrons is projected out because of the strong on-site repulsion, and this constitutes the strong correlation physics. We can represent these states in terms of canonical operators by decomposing the electron operator into spinon and holon operators. On one sublattice of the square lattice we write the electron operator, c_α as

$$c_\alpha = b_\alpha f_+^\dagger \quad (A1)$$

where b_α are canonical ‘Schwinger’ bosons and f_+ are canonical fermionic holons. The projection onto the 3 allowed states is imposed by the local constraint

$$f_+^\dagger f_+ + b^{\alpha\dagger} b_\alpha = 1 \quad (A2)$$

on each site. On the other sublattice, we use bosons which transform as a conjugate representation

$$c_\alpha = \varepsilon_{\alpha\beta} \bar{b}^\beta f_-^\dagger \quad (A3)$$

with a similar constraint.

Now consider the mean-field U(1) spin liquid state of the insulator. This is described by the effective Hamiltonian^{16,17}

$$H_J = -Q \sum_{\langle ij \rangle} b_{i\alpha} \bar{b}_j^\alpha + \text{H.c.} + \lambda \sum_i b_i^{\alpha\dagger} b_{i\alpha} + \lambda \sum_j \bar{b}_{j\alpha}^\dagger \bar{b}_j^\alpha, \quad (A4)$$

where i is restricted to be on one sublattice, and j on the other, and Q , λ are positive constants. Any operation which interchanges the two sublattices leaves H_J invariant under

the PSG mapping

$$\begin{aligned} b_\alpha &\rightarrow \varepsilon_{\alpha\beta} \bar{b}^\beta \\ \bar{b}^\alpha &\rightarrow \varepsilon^{\alpha\beta} b_\beta. \end{aligned} \quad (\text{A5})$$

Further, the invariances of Eqs. (A1,A3) under such an operation demand that

$$\begin{aligned} f_+ &\rightarrow f_- \\ f_- &\rightarrow -f_+. \end{aligned} \quad (\text{A6})$$

Note especially the sign in the last equation, which is a consequence of $\varepsilon^{\alpha\beta}\varepsilon_{\beta\gamma} = -\delta_\gamma^\alpha$.

The spinon spectrum of H_J shows that the minimum energy excitations are near zero momentum, and so we may take its low energy limit by a naive gradient expansion. This leads¹⁷ to the effective theory \mathcal{L}_z in Eq. (2) with

$$z_\alpha \sim b_\alpha + \bar{b}_\alpha^\dagger \quad (\text{A7})$$

The PSG of the z_α in Table I follows from the above relations.

Determination of the PSG of the f_{qv} requires the additional information that the holons have their dispersion minima $\vec{K}_{1,2}$. The phase factors associated with the transformation properties of $e^{i\vec{K}_v \cdot \vec{r}}$, combined with those in Eq. (A6) lead to the results in Table I.

APPENDIX B: HOLES IN THE NÉEL STATE

By spin rotation invariance, we can always rotate the z_α condensate (and without *any* rotation of the spinless f_{qv}) to produce a Néel order $N^a = z^{\alpha*}\sigma_\alpha^{a\beta}z_\beta$ (where σ^a are the Pauli matrices) polarized along the $(0, 0, 1)$ direction. Now examine the response of the theory to a uniform magnetic field H applied along the z direction. Under such a field, the only change in the action is that¹⁵ $(\partial_\tau - iA_\tau)z_\alpha \rightarrow (\partial_\tau - iA_\tau + (H/2)\sigma^z)z_\alpha$. Choosing $\langle z_\alpha \rangle = \sqrt{|s - s_c|/u}\delta_{\alpha\uparrow}$, we obtain a term in the Lagrangian

$$\mathcal{L} = \dots (|s - s_c|/u) [iA_\mu - (H/2)\delta_{\mu\tau}]^2 + \dots \quad (\text{B1})$$

which gaps the A_μ photon. Integrating out the A_μ and then evaluating $M_z = \delta\mathcal{S}/\delta H|_{H=0}$, we obtain an expression for the magnetization density M_z

$$M_z = \frac{1}{2} \sum_{qv} q f_{qv}^\dagger f_{qv} + \dots \quad (\text{B2})$$

where the ellipses represent an additional term which measures the magnetization of the spin waves. This establishes, as claimed in Fig. 1, that $S_z = q/2$ for the fermions in the Néel phase.

APPENDIX C: HOLON-SPINON BOUND STATES

We describe the structure of a holon-spinon bound state in more detail. The bound state of a f_{+1} holon with a spinon will be mixed by \mathcal{L}_c with the bound state of a f_{-1} holon with a spinon (parallel considerations apply to the $f_{\pm 2}$ holons).

Before writing the wave-function for this bound state, we need to decompose the relativistic field z_α into non-relativistic, canonical boson fields p_α (the spinon) and h_α (the anti-spinon). At low momenta, this is done by the standard parameterization

$$z_\alpha = \frac{1}{\sqrt{2\Delta}} (p_\alpha + \varepsilon_{\alpha\beta} h^{\beta\dagger}) \quad (\text{C1})$$

In the absence of \mathcal{L}_c the bound state of f_{+1} and h_α and the bound state of f_{-1} and p_α are independent, and thus the problem can be solved in the familiar center-of-mass frame,

$$M_{\bar{j}} = m_{v\bar{j}} + \Delta; \quad R_{\bar{j}} = \frac{m_{v\bar{j}} r_{h\bar{j}} + \Delta r_{s\bar{j}}}{m_{v\bar{j}} + \Delta} \quad (\text{C2})$$

$$\rho_{\bar{j}} = \frac{m_{v\bar{j}} \Delta}{m_{v\bar{j}} + \Delta}; \quad \vec{r} = \vec{r}_h - \vec{r}_s \quad (\text{C3})$$

Δ is the mass of the spinon in the non-relativistic limit, and $m_{v\bar{j}}$ are the holon masses in \mathcal{L}_f . The holon co-ordinate is represented by \vec{r}_h and that of the spinon by \vec{r}_s . The kets describing the motion of the bound state can be labeled in terms of the momentum \vec{P} of the bound state center-of-mass,

$$\begin{aligned} |\alpha \vec{P}+\rangle &= \int d\vec{r}_S d\vec{r}_h e^{i\vec{P}\cdot\vec{R}} \phi(\vec{r}) f_{+1}^\dagger(\vec{r}_h) h^{\alpha\dagger}(\vec{r}_s) |0\rangle \\ |\alpha \vec{P}-\rangle &= \int d\vec{r}_S d\vec{r}_h e^{i\vec{P}\cdot\vec{R}} \phi(\vec{r}) f_{-1}^\dagger(\vec{r}_h) p^{\alpha\dagger}(\vec{r}_s) |0\rangle \end{aligned} \quad (\text{C4})$$

The kets correspond to the eigenvalues $E_{\vec{P}}^0 = \frac{P_{\bar{j}}^2}{2M_{\bar{j}}}$ and have been written in terms of the “first-quantized” ground state wavefunction $\phi(r)$ of the holon-spinon interaction, $V(r)$. $V(r) = (12\Delta/N) \ln(r\Delta)$ binds the holons and spinons over a length scale $\sim 1/\Delta$, with $\phi(0) \sim \Delta$.

The mixing of the \pm kets due to \mathcal{L}_c can be studied by interpreting this term simply as a Hamiltonian \mathcal{H}_c with the operator identification in Eq. (C1). \mathcal{H}_c only connects kets with

the same \vec{P} and α with the matrix element $\langle \alpha \vec{P} + |\mathcal{H}_c| \alpha \vec{P} - \rangle = -\frac{\tilde{\lambda}|\phi(0)|^2 P_{\bar{x}}}{M_x}$ (we used the fact that $\partial_x \phi(0) = 0$). Now, by simply diagonalizing a 2×2 matrix we can infer the dispersion $E_{\vec{P}}$ induced by \mathcal{L}_c to first order in perturbation theory in $\tilde{\lambda}$,

$$E_{\vec{P}}^1 = \frac{P_{\bar{i}}^2}{2M_{\bar{i}}} \pm \frac{\tilde{\lambda}P_{\bar{x}}|\phi(0)|^2}{M_x} \quad (\text{C5})$$

with eigenmodes which correspond precisely to the electron states in Eq. (3) (x is replaced by y for $f_{\pm 2}$). So the bound state dispersion has a minimum at $K_{\bar{x}} = \pm \lambda$ where $\lambda = \tilde{\lambda}|\phi(0)|^2 \sim \Delta^2$. This is responsible for the shift in the centers of the elliptical hole pockets shown in Fig 2.

APPENDIX D: COUPLING TO VBS ORDER

Here we describe the terms in action which couple the VBS order parameter Φ_{VBS} to the holons and/or spinons. Such terms are responsible for the mixing between the Fermi surfaces of the VBS state (shown in Fig. 2) and the ‘shadow’ Fermi surfaces obtained by Bragg reflection across the reduced Brillouin zone boundaries (shown as dashed lines).

The most general terms in the action follow by the requirements that they be U(1) gauge invariant, and also invariant under the PSG in Table 1. These requirements turn out to be extremely restrictive.

First, we search for terms which involve Φ_{VBS} and a bilinear of the f_{qv} fermions. However a detailed analysis shows that there *no such terms* which are invariant under all the PSG operations; this is seen by first listing the f_{qv} bilinear invariants under I_x^{dual} (under which Φ_{VBS} is invariant), and then noting that their transformations under $R_{\pi/2}^{\text{dual}}$ are incompatible with those of Φ_{VBS} . Consequently, the coupling between the VBS order and the fermions will be weaker than might have been initially expected, and will vanish faster than $\langle \Phi_{\text{VBS}} \rangle \sim \Delta^{\beta_{\text{VBS}}/\nu}$ as $\Delta \rightarrow 0$.

The simplest non-vanishing coupling turns out to require the full Ψ_p electron operators in Eq. (3). This has the form

$$\begin{aligned} \mathcal{L}_{\text{VBS}} = \lambda_{\text{VBS}} \Phi_{\text{VBS}}^* & \left[-i(\Psi_1^\dagger \Psi_4 - \Psi_4^\dagger \Psi_1 + \Psi_2^\dagger \Psi_3 - \Psi_3^\dagger \Psi_2) \right. \\ & \left. + (\Psi_1^\dagger \Psi_2 - \Psi_2^\dagger \Psi_1 + \Psi_4^\dagger \Psi_3 - \Psi_3^\dagger \Psi_4) \right] + \text{c.c.} \end{aligned} \quad (\text{D1})$$

Now we need an estimate of the matrix element of \mathcal{L}_{VBS} between the holon-spinon bound states found in the previous section. Using Eqs. (C1) and (C4), we obtain a matrix element of order

$$\lambda_{\text{VBS}} \langle \Phi_{\text{VBS}} \rangle \frac{|\phi(0)|^2}{\Delta} \sim \lambda_{\text{VBS}} \Delta^{1+\beta_{\text{VBS}}/\nu}. \quad (\text{D2})$$

As expected, this does vanish faster than $\Delta^{\beta_{\text{VBS}}/\nu}$, and is responsible for the weak Bragg reflection across the reduced Brillouin zone boundaries of the VBS state in Fig. 2.

¹ P. Coleman and A. J. Schofield, *Nature* **433**, 226 (2005).

² Q. Si, *cond-mat/0601001*.

³ T. Senthil, S. Sachdev, and M. Vojta, *Physica B* **359-361**, 9 (2005); T. Senthil, *Annals of Physics*, **321**, 1669 (2006).

⁴ A. Kanigel, M. R. Norman, M. Randeria, U. Chatterjee, S. Suoma, A. Kaminski, H. M. Fretwell, S. Rosenkranz, M. Shi, T. Sato, T. Takahashi, Z. Z. Li, H. Raffy, K. Kadowaki, D. Hinks, L. Ozyuzer, and J. C. Campuzano, *Nature Physics* **2**, 447 (2006).

⁵ H. Shishido, R. Settai, H. Harima, and Y. Onuki, *J. Phys. Soc. Jpn.* **74**, 1103 (2005).

⁶ T. Senthil, A. Vishwanath, L. Balents, S. Sachdev, and M. P. A. Fisher, *Science* **303**, 1490 (2004); T. Senthil, L. Balents, S. Sachdev, A. Vishwanath, and M. P. A. Fisher, *Phys. Rev. B* **70**, 144407 (2004).

⁷ T. Senthil, S. Sachdev, and M. Vojta, *Phys. Rev. Lett.* **90**, 216403 (2003); T. Senthil, M. Vojta, and S. Sachdev, *Phys. Rev. B* **69**, 035111 (2004).

⁸ Q. Si, S. Rabello, K. Ingersent, and J. L. Smith, *Nature* **413**, 804 (2001).

⁹ M. Levin and T. Senthil, *Phys. Rev. B* **70**, 220403 (2004).

¹⁰ A. Kuklov, N. Prokof'ev, B. Svistunov, and M. Troyer, *Annals of Physics* **321**, 1602 (2006) have studied a particular lattice realization of the ‘easy-plane’ limit of the field theory proposed in Ref. 6, and found a first-order transition. This does not rule out a second-order transition for other lattice realizations. A second-order, deconfined, transition has been theoretically established for N sufficiently large, but finite. There is also strong numerical evidence for a continuous transition for the physically interesting case with $N = 2$ and full $SU(2)$ symmetry^{11,12,13}.

¹¹ A. W. Sandvik, *cond-mat/0611343*.

¹² M. Kamal and G. Murthy, *Phys. Rev. Lett.* **71**, 1911 (1993).

¹³ O. I. Motrunich and A. Vishwanath, Phys. Rev. B **70**, 075104 (2004).

¹⁴ M. Hermele, T. Senthil, M. P. A. Fisher, P. A. Lee, N. Nagaosa, and X.-G. Wen, Phys. Rev. B **70**, 214437 (2004).

¹⁵ A. Kolezhuk, S. Sachdev, R. R. Biswas, and P. Chen, Phys. Rev. B **74**, 165114 (2006).

¹⁶ D. P. Arovas and A. Auerbach, Phys. Rev. B **38**, 316 (1988).

¹⁷ N. Read and S. Sachdev, Phys. Rev. Lett. **62**, 1694 (1989).

¹⁸ C. L. Kane, P. A. Lee, and N. Read, Phys. Rev. B **39**, 6880 (1989).

¹⁹ Y. M. Li, D. N. Sheng, Z. B. Su, and L. Yu, Phys. Rev. B **45**, 5428 (1992).

²⁰ X.-G. Wen, Phys. Rev. B **65**, 165113 (2002).

²¹ B. I. Shraiman and E. D. Siggia, Phys. Rev. Lett. **61**, 468 (1988).

²² F. Kämpfer, M. Moser, and U.-J. Wiese, Nucl. Phys. B **729**, 317 (2005); C. Brügger, F. Kämpfer, M. Moser, M. Pepe, and U.-J. Wiese, cond-mat/0606766.

²³ G. Murthy and S. Sachdev, Nucl. Phys. B **344**, 557 (1990).

²⁴ W. Rantner and X.-G. Wen, cond-mat/02101521.

²⁵ H. Kleinert and A. M. J. Schakel, Phys. Rev. Lett. **90**, 097001 (2003).

²⁶ M. T. Béal-Monod and K. Maki, Phys. Rev. Lett. **34**, 1461 (1975); J. A. Hertz, Phys. Rev. B **14**, 1165 (1976); A. J. Millis, Phys. Rev. B, **48**, 7183 (1993).

²⁷ A. Georges, G. Kotliar, W. Krauth, and M. Rozenberg, Rev. Mod. Phys. **68**, 13 (1996).